

by using the method developed by Huheey.<sup>13</sup> It can be seen that as in the case of atoms group electronegativity values are also reproduced well. It can also be seen that the charge coefficients are well correlated with Huheey's values. Note, for example, CF<sub>3</sub> vs. CF<sub>2</sub>CF<sub>3</sub>; even though the electronegativity values are similar for both species the charge coefficients vary. But they do so in exactly the same manner in both schemes. One case in which the two schemes consistently differ is with regard to the charge coefficient of H containing groups. It can be seen that Huheey's values are greater in all cases considered. The reason for the difference lies in the different values for the charge coefficient for the H atom in each scheme (Huheey = 4.32, present method = 3.12). In these cases Huheey's values are expected to correlate better with experimental data since they are based on measured values for ionization potential and electron affinity for H.

### Summary

A general relation, i.e., (32), has been derived which can be used to calculate electronegativity of any atomic orbital in any bonding situation. In the case of neutral atoms all  $\delta_{A,i}$  of (32)

are equal to 0 and (32) reduces to (22). In the case of groups the  $\delta_{A,i}$  values are in general not equal to 0 for the bonded orbitals. In order to calculate group electronegativity these  $\delta_{A,i}$  values must be evaluated. To do this two constraints must be placed on each bond (since there are two unknowns per A-B bond, i.e.,  $\delta_{A,i}$  and  $\delta_{B,i}$ ). In the present paper these are chosen as the conservation of charge, i.e.,  $\delta_{A,i} + \delta_{B,i} = 0$ , and the electronegativity equilibration principle, i.e.,  $\chi_A(\delta_{A,i}) = \chi_B(\delta_{B,i})$ . Once the  $\delta_{A,i}$  values are calculated, they are substituted into (32 along with  $\delta_{A,i} = 0$  (i.e., the orbital to be bonded has one electron prior to bonding) to give the group electronegativity. This formalism also leads to a very simple relation (equation 45) that can be used to calculate the electronegativity of groups in which each atom utilizes the same type of orbital for each of its bonds.

With these relations both atomic and group electronegativities are easily calculable in terms of orbital hybridization and modified Slater's screened nuclear charge and effective principal quantum number. Not only is the method simple to use but it is also readily related to theoretical concepts and thus can be made more precise as well as being useful in a wider area.

## Carbene and Silylene Insertion Reactions. Ab Initio Calculations on the Effects of Fluorine Substitution

Carlos Sosa and H. Bernhard Schlegel\*

Contribution from the Department of Chemistry, Wayne State University, Detroit, Michigan 48202. Received February 3, 1984

**Abstract:** The insertion reactions of CH<sub>2</sub>, CHF, CF<sub>2</sub>, SiH<sub>2</sub>, SiHF, and SiF<sub>2</sub> into hydrogen molecule have been investigated by ab initio molecular orbital methods. Reactants, loose clusters, transition structures, and products were optimized at HF/3-21G and HF/6-31G\*. For each structure, relative energies have been calculated at MP4SDQ/6-31G\* and vibrational frequencies at HF/3-21G. A dramatic increase in the barrier height is seen with fluorine substitution: 8, 64, and 197 and 51, 130, and 273 kJ mol<sup>-1</sup> for CH<sub>2</sub>, CHF, and CF<sub>2</sub> and SiH<sub>2</sub>, SiHF, and SiF<sub>2</sub>, respectively, at MP4SDQ/6-31G\*/HF/6-31G\* plus  $\Delta ZPE$ . An orbital interaction interpretation is given for the trend in barrier heights, and implications for the chemistry of carbenes and silylenes are discussed.

Carbenes have long attracted the attention of experimentalists<sup>1</sup> and theoreticians.<sup>2,3</sup> For silylenes, there has recently been a surge of interest, both as second-row analogues of carbenes and as reactive intermediates in organosilicon chemistry.<sup>4</sup> A wide variety of silylenes can be generated by flash photolysis and vacuum pyrolysis of silanes, halosilanes, and alkylsilanes.<sup>4</sup> Silylenes are also thought to be important constituents in the chemical vapor deposition of amorphous silicon films from SiH<sub>4</sub><sup>5</sup> and possibly also from SiF<sub>4</sub>. In addition, silylenes can be formed by rearrangement of unsaturated and/or cyclic organosilicon compounds,<sup>6</sup> because of silicon's reluctance to form multiple bonds, such rearrangement are often thermoneutral or exothermic.<sup>7</sup>

The parent silylene, SiH<sub>2</sub>, and simple substituted silylenes (SiHX, X = OH, F, Cl, Br, I, CH<sub>3</sub>, SiH<sub>3</sub>; SiX<sub>2</sub>, X = F, Cl, Br, I) have been studied experimentally in some detail.<sup>8</sup> The ground states are invariably closed shell singlets with sharply bent geometries ( $\angle XSiY$  ca. 95°); some excited-state singlets and triplets have also been characterized.<sup>8</sup> Vibrational frequencies are available for ground and excited states of SiH<sub>2</sub>, SiHF, and SiF<sub>2</sub> (among others) from matrix isolation studies and electronic spectra.<sup>13-15</sup> Schaefer et al.<sup>16</sup> have recently carried out extensive ab initio calculations on these species and obtained excellent agreement with experiment.

Once formed, silylenes can react by abstraction, dimerization, disproportionation, cycloaddition, and insertion.<sup>4</sup> Insertion re-

actions of SiH<sub>2</sub> have been observed with H<sub>2</sub>, Si-H, and Si-Si bonds. In contrast, SiF<sub>2</sub> is surprisingly inert in the gas phase,<sup>9</sup>

- (1) Moss, R. A.; Jones, M., Jr. In "Reactive Intermediates"; Jones, M., Jr., Eds.; Wiley-Interscience: New York, 1981; Vol. 2, pp 59-133.
- (2) For a review, see: Borden, W. T.; Davidson, E. R. *Annu. Rev. Phys. Chem.* **1979**, *30*, 125.
- (3) For examples of carbene insertions, particularly CH<sub>2</sub> + H<sub>2</sub>, see: Cain, S. R.; Hoffmann, R.; Grant, E. R. *J. Phys. Chem.* **1981**, *85*, 4046. Kollmar, H.; Staemmler, V. *Theor. Chim. Acta* **1979**, *51*, 207. Jeziorek, D.; Zurawski, B. *Int. J. Quantum Chem.* **1979**, *16*, 277. Bauschlicher, C. W., Jr.; Haber, K.; Schaefer, H. F., III; Bender, C. F. *J. Am. Chem. Soc.* **1977**, *99*, 3610 and references cited.
- (4) Gaspar, P. P. In "Reactive Intermediates"; Jones, M., Jr., Moss, R. A., Eds.; Wiley-Interscience: New York, 1981; Vol. 2, pp 335-385.
- (5) Scott, B. A.; Plecenik, R. M.; Simonyi, E. E.; *Appl. Phys. Lett.* **1981**, *39*, 73. Haller, I. *J. Vac. Sci. Technol.* **1983**, *1*, 1376.
- (6) Reisenauer, H. P.; Mihm, G.; Maier, G. *Angew. Chem., Int. Ed. Engl.* **1982**, *21*, 854. Burns, S. A.; Burns, G. T.; Barton, T. J. *J. Am. Chem. Soc.* **1982**, *104*, 6140.
- (7) Walsh, R. *Acc. Chem. Res.* **1981**, *14*, 246.
- (8) For leading references see ref 8-14.
- (9) Margrave, J. L.; Wilson, P. W. *Acc. Chem. Res.* **1971**, *4*, 145.
- (10) Lee, H. U.; DeNeufville, J. P. *Chem. Phys. Lett.* **1983**, *99*, 394.
- (11) Dubois, I. *Can. J. Phys.* **1968**, *46*, 2485.
- (12) Rao, V. M.; Curl, R. F.; Timms, P. L.; Margrave, J. L. *J. Chem. Phys.* **1965**, *43*, 2557.
- (13) Milligan, D. E.; Jacox, M. E. *J. Chem. Phys.* **1970**, *52*, 2594.
- (14) Ismail, Z. K.; Fredin, L.; Hauge, R. H.; Margrave, J. L. *J. Chem. Phys.* **1982**, *77*, 1626.
- (15) Caldwell, G. L.; Deely, C. M.; Turner, P. H.; Mills, I. M. *Chem. Phys. Lett.* **1981**, *82*, 434.

\* Fellow of the Alfred P. Sloan Foundation, 1981-83.

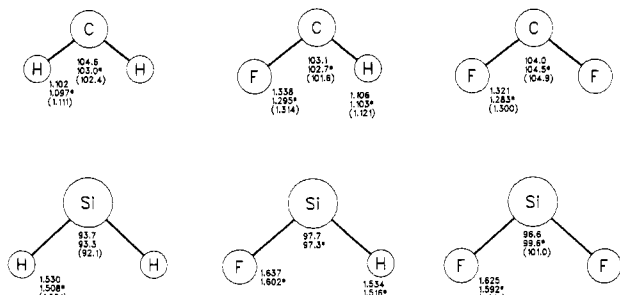


**Figure 1.** Geometries of carbene and silylene and their mono- and difluoro derivatives: HF/3-21G optimized (no superscript), HF/6-31G\* optimized (asterisk), and experimental<sup>11,12,30</sup> (parentheses) in Å and degrees.

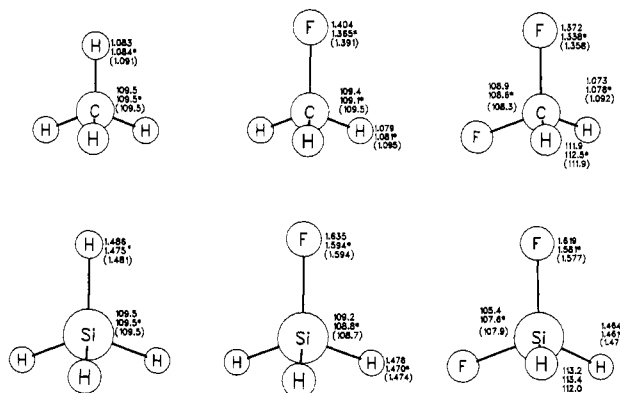


**Figure 2.** Geometries for the products of the carbene and silylene insertion reactions: HF/3-21G optimized (no superscript), HF/6-31G\* optimized (asterisk), and experimental<sup>32</sup> (parentheses) in Å and degrees.

although quite reactive in condensed phases. Theoretical studies of silylene reactions have so far been limited to rearrangements<sup>17</sup> (1,2 shifts), forming the related unsaturated structures, and to insertion reactions of unsubstituted silylene.<sup>18-21</sup> For  $\text{SiH}_2 + \text{H}_2$ , the theoretical barrier heights, 36.0 kJ mol<sup>-1</sup> calculated by Gordon<sup>18</sup>, and 27.9 kJ mol<sup>-1</sup> calculated by Schaefer,<sup>19</sup> are in good agreement with the experimental value of  $23 \pm 4$  kJ mol<sup>-1</sup> measured by John and Purnell.<sup>22</sup> Silylene insertion into first- and second-row hydrides have also been studied<sup>20,21</sup> and possess barriers of 10–50 kJ mol<sup>-1</sup>. By comparison,  $\text{CH}_2 + \text{H}_2$  insertion has no barrier.<sup>1-3</sup>

In this paper we use ab initio calculations to explore the effect of fluorine substitution on the insertion of silylene into hydrogen molecule. We have also carried out a parallel study on fluoro-carbene insertions. Although the singlet  $\text{CH}_2 + \text{H}_2 \rightarrow \text{CH}_4$  reaction has been well studied theoretically,<sup>3</sup> only a few ab initio calculations are available for the effect of substituents on the transition structure for insertion<sup>23</sup> or cycloaddition.<sup>24</sup>

## Method

Ab initio molecular orbital calculations were performed with the GAUSSIAN 80 and 82 systems,<sup>25</sup> using extended<sup>26a</sup> (3-21G) and polariza-

(16) Colvin, M. E.; Grev, R. S.; Schaefer, H. F., III; Bicerano, J. *Chem. Phys. Lett.* **1983**, *99*, 399.

(17) For reviews see: Schaefer, H. F., III, *Acc. Chem. Res.* **1982**, *15*, 283. Kohler, H. J.; Lischka, H. *J. Am. Chem. Soc.* **1982**, *104*, 5884.

(18) Gordon, M. S. *J. Chem. Soc., Chem. Commun.* **1981**, 890.

(19) Grev, R. S.; Schaefer, H. F., III, *J. Chem. Soc., Chem. Commun.* **1983**, 785.

(20) Raghavachari, K.; Chandrasekhar, J.; Frisch, M. J. *J. Am. Chem. Soc.* **1982**, *104*, 3779.

(21) Gordon, M.; Gano, D. R. *J. Am. Chem. Soc.*, in press. Raghavachari, K.; Chandrasekhar, J.; Gordon, M. S.; Dykema, K. *J. Am. Chem. Soc.*, in press.

(22) John, P.; Purnell, J. H. *J. Chem. Soc., Faraday Trans. 1* **1973**, *69*, 1455.

(23) Harding, L. B.; Schlegel, H. B.; Krishnan, R.; Pople, J. A. *J. Phys. Chem.* **1980**, *84*, 3394.

(24) Rondan, N. G.; Houk, K. N.; Moss, R. A. *J. Am. Chem. Soc.* **1980**, *102*, 1770.

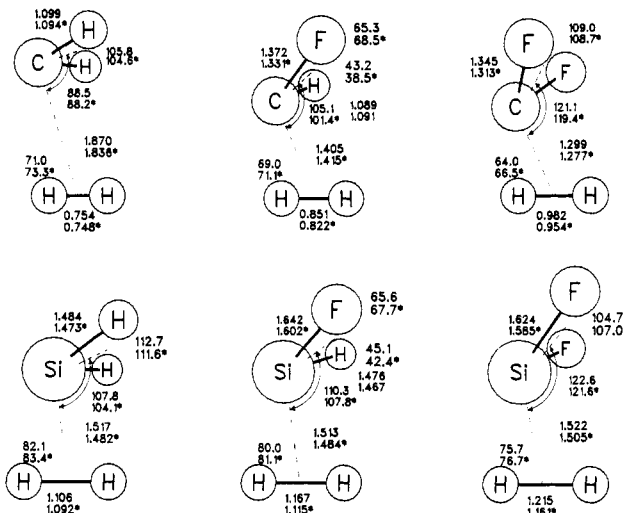


**Figure 3.** Transition structures for the carbene and silylene insertion reactions optimized at HF/3-21G (no superscript) and HF/6-31G\* (asterisk). For CHF, the F-C-X-H<sub>2</sub> dihedral angle is 98.9°, 99.4°, where X is a dummy atom in the CHF and C-H<sub>2</sub> planes. Similarly for SiHF, F-Si-X-H<sub>2</sub> is 101.7°, 102.4°.

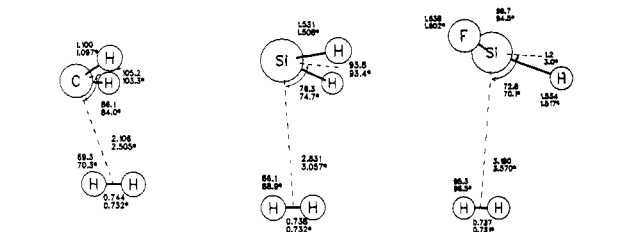


**Figure 4.** Loose molecular clusters along the reaction path to insertion optimized at HF/3-21G (no superscript) and HF/6-31G\* (asterisk). For SiHF, the F-Si-X-H<sub>2</sub> dihedral angle is ca. 90° and ca. 90°.

tion<sup>26a</sup> (6-31G\*) basis sets. All equilibrium geometries and transition structures were fully optimized with analytical gradient methods<sup>27</sup> at the Hartree-Fock level. Electron correlation energy was estimated by using Møller-Plesset perturbation theory<sup>28</sup> up to fourth order, including all single, double, and quadruple excitations (MP4SDQ, frozen core). Vibrational frequencies and zero-point energies were obtained from analytical second derivatives<sup>29</sup> calculated at the HF/3-21G level.

## Results

**Geometry.** The experimental and theoretical structures for the reactant carbenes and silylenes are collected in Figure 1; the product geometries are summarized in Figure 2. The present computations are in good agreement with the more extensive MCSCF calculations by Schaefer et al.<sup>16,33</sup> As has already been

(25) Binkley, J. S.; Whiteside, R. A.; Krishnan, R.; Seeger, R.; DeFrees, D. J.; Schlegel, H. B.; Topiol, S.; Kahn, R. L.; Pople, J. A. *QCPE* **1980**, *13*, 406.

(26) (a) Binkley, J. S.; Pople, J. A.; Hehre, W. J. *J. Am. Chem. Soc.* **1980**, *102*, 939. Gordon, M. S.; Binkley, J. S.; Pople, J. A.; Pietro, W. J.; Hehre, W. J. *Ibid.* **1982**, *104*, 2797. (b) Hariharan, P. C.; Pople, J. A. *Theor. Chem. Acta.* **1973**, *28*, 213 and references cited. Francl, M. M.; Pietro, W. J.; Hehre, W. J.; Binkley, J. S.; Gordon, M. S.; DeFrees, D. J.; Pople, J. A. *J. Chem. Phys.* **1982**, *77*, 3654 and references cited.

(27) Schlegel, H. B. *J. Comput. Chem.* **1982**, *3*, 214.

(28) Krishnan, R.; Pople, J. A. *Int. J. Quantum Chem., Quantum Chem. Symp.* **1980**, *14*, 91.

(29) Pople, J. A.; Krishnan, R.; Schlegel, H. B.; Binkley, J. S. *Int. J. Quantum Chem., Quantum Chem. Symp.* **1979**, *13*, 225. Pople, J. A.; Schlegel, H. B.; Krishnan, R.; DeFrees, D. J.; Binkley, J. S.; Frisch, M. J.; Whiteside, R. A.; Hout, R. F.; Hehre, W. J. *Ibid.* **1981**, *15*, 269.

(30) (a) Herzberg, G. "Electronic Spectra of Polyatomic Molecules"; Van Nostrand: Princeton, 1967. (b) Merer, A. J.; Travis, D. N. *Can. J. Phys.* **1966**, *44*, 1514. (c) Mathews, C. W. *Ibid.* **1967**, *45*, 524.

(31) (a) Herzberg, G.; Johns, J. W. C. *Proc. R. Soc. London, Ser. A* **1966**, *107*, 295. Petek, H.; Nesbitt, D. J.; Ogilby, P. R.; Moore, C. B. *J. Phys. Chem.* **1983**, *87*, 5367. (b) Jacox, M. E.; Milligan, D. E. *J. Chem. Phys.* **1969**, *50*, 3252. (c) Milligan, D. E.; Mann, D. E.; Jacox, M. E. *Ibid.* **1964**, *41*, 1199.

(32) Stull, D. R.; Prophet, H. "IANAF Thermochemical Tables"; U. S. Government Printing Offices: Washington DC, 1971 and subsequent supplements.

Table I. Vibrational Frequencies<sup>a</sup>

| CH <sub>2</sub> + H <sub>2</sub> | CHF + H <sub>2</sub> | CF <sub>2</sub> + H <sub>2</sub> | SiH <sub>2</sub> + H <sub>2</sub> | SiHF + H <sub>2</sub> | SiF <sub>2</sub> + H <sub>2</sub> |
|----------------------------------|----------------------|----------------------------------|-----------------------------------|-----------------------|-----------------------------------|
| Reactants                        |                      |                                  |                                   |                       |                                   |
| 1561 (1353)                      | 1268 (1182)          | 676 (668)                        | 1107 (1005)                       | 920 (834)             | 377 (345)                         |
| 3034 (2806)                      | 1520 (1405)          | 1280 (1110)                      | 2063                              | 965 (859)             | 958 (855)                         |
| 3089 (2865)                      | 2965 (2918)          | 1322 (1222)                      | 2078 (2022)                       | 2046 (1913)           | 971 (872)                         |
| Transition Structures            |                      |                                  |                                   |                       |                                   |
| 225i a'                          | 1324i                | 1932i a'                         | 1715i a'                          | 1796i                 | 2011i a'                          |
| 603 a''                          | 779                  | 564 a'                           | 825 a'                            | 636                   | 342 a'                            |
| 764 a'                           | 1104                 | 805 a'                           | 866 a''                           | 772                   | 604 a''                           |
| 863 a''                          | 1157                 | 869 a''                          | 982 a'                            | 848                   | 721 a'                            |
| 1107 a'                          | 1259                 | 1172 a'                          | 1114 a''                          | 943                   | 934 a'                            |
| 1539 a'                          | 1496                 | 1298 a''                         | 1585 a'                           | 1150                  | 1004 a''                          |
| 3065 a'                          | 1772                 | 1418 a''                         | 2123 a'                           | 1475                  | 1046 a''                          |
| 3139 a''                         | 2907                 | 1733 a'                          | 2289 a'                           | 2197                  | 1335 a'                           |
| 4270 a'                          | 3180                 | 2644 a'                          | 2308 a''                          | 2355                  | 2329 a'                           |
| Products                         |                      |                                  |                                   |                       |                                   |
| 1520 (1306)                      | 1143 (1049)          | 534 (529)                        | 973 (913)                         | 800 (728)             | 341 (322)                         |
| 1740 (1534)                      | 1278 (1182)          | 1182 (1090)                      | 1046 (972)                        | 943 (875)             | 782 (730)                         |
| 3187 (2917)                      | 1663 (1464)          | 1250 (1116)                      | 2286 (2186)                       | 990 (961)             | 805 (730)                         |
| 3280 (3019)                      | 1686 (1467)          | 1262 (1176)                      | 2295 (2189)                       | 1132 (991)            | 934 (869)                         |
|                                  | 3228 (2965)          | 1401 (1262)                      |                                   | 2338 (2209)           | 996 (903)                         |
|                                  | 3293 (3006)          | 1639 (1435)                      |                                   | 2352 (2206)           | 1041 (982)                        |
|                                  |                      | 1733 (1508)                      |                                   |                       | 1127 (981)                        |
|                                  |                      | 3300 (2949)                      |                                   |                       | 2429 (2251)                       |
|                                  |                      | 3363 (3013)                      |                                   |                       | 2435 (2246)                       |

<sup>a</sup> In cm<sup>-1</sup>, theoretical harmonic frequencies computed at HF/3-21G; observed anharmonic frequencies in parentheses from ref 31 (carbenes), 13-15 (silylenes), and 32 (fluoromethanes and silanes).

established, the 3-21G basis set overestimates the C-F bond lengths,<sup>26a</sup> while the HF/6-31G\* level underestimates them.<sup>26b</sup> The Si-F bond is also too long with the 3-21G basis but in good agreement with experiment at the HF/6-31G\* level. Except for  $\angle$ FSiF, the bond angles are not affected significantly by changes in the basis set. The increase in the F-Si-F angle on going from 3-21G to 6-31G\* is probably due to the shortening of the SiF bonds, leading to greater F-F repulsion.

The optimized geometries for the transition structures are presented in Figure 3. Note that at higher levels of calculation,<sup>3</sup> there is no barrier for CH<sub>2</sub> + H<sub>2</sub> → H<sub>2</sub> and hence no transition structure. The CHF + H<sub>2</sub> saddle point is very similar to HCOH + H<sub>2</sub>, both in terms of distances and orientation.<sup>23</sup> The SiH<sub>2</sub> + H<sub>2</sub> transition structure agrees well with the SCF calculations of Gordon<sup>18</sup> and the MCSCF geometry optimization of Schaefer.<sup>19</sup> Within the carbene and silylene fragments, the agreement between the 3-21G and 6-31G\* structures is similar to the ground state. Somewhat larger variations are found for the distances and angles between the H<sub>2</sub> and carbene or silylene fragments (0.02-0.03 Å shortening and ±2° change, on going from 3-21G to 6-31G\*).

A comparison of the six transition structures yields a number of trends. The silylene insertions show a larger increase in the H<sub>2</sub> bond length (ground state H<sub>2</sub>,  $R = 0.735$  Å at 3-21G and 0.730 Å at 6-31G\*) and a greater opening of the silylene valence angle. Increasing the number of fluorines causes a large decrease in the carbene-H<sub>2</sub> distance but leaves the silylene-H<sub>2</sub> distance relatively unaffected. Fluorine substitution also increases the H-H distance, decreases the HX<sub>1</sub>C and HX<sub>1</sub>Si angles (where X<sub>1</sub> is the midpoint of the H-H bond), and increases  $\angle$ X<sub>1</sub>CX<sub>2</sub> and  $\angle$ X<sub>1</sub>SiX<sub>2</sub> (where X<sub>2</sub> is on the carbene or silylene valence angle bisector). All three features indicate that the transition structure occurs progressively later along the reaction path for insertion as the fluorine substitution is increased. This is in agreement with Hammond's postulate, since fluorine substitution also decreases the exothermicity of the insertion reactions.

Further out along the reaction path, we were able to locate loose clusters for three of the systems (Figure 4). In each case, the binding energy is very small and the monomer geometries are essentially unperturbed (at higher levels of calculation, the CH<sub>2</sub> + H<sub>2</sub> cluster does not exist; see below). The carbene and silylene

fragments are oriented with their plane parallel to the H<sub>2</sub> axis. For silylene, fluorine substitution causes a large increase in the distance between the monomers. The corresponding SiF<sub>2</sub> + H<sub>2</sub> structure (not shown) has  $R = 3.5$  Å at HF/3-21G; however, it has an imaginary frequency, i.e., is a saddle point, with respect to the relative orientation of H<sub>2</sub> and SiF<sub>2</sub>. Other loosely bound carbene and silylene + H<sub>2</sub> clusters with different structures no doubt exist but are probably not relevant to the insertion reactions.

**Frequencies.** The HF/3-21G harmonic frequencies are collected in Table I and are compared with experimental (anharmonic) frequencies, where available. The computed frequencies are ca. 10% to high due to the neglect of vibrational anharmonicity and electron correlation.<sup>29</sup> The present theoretical values for carbene and silylene are in good agreement with larger basis set calculations carried out by Schaefer et al.<sup>16</sup> In the loose clusters (not listed), the carbene and silylene frequencies are shifted by less than ±1%; in addition there are five low-frequency vibrations for the relative motion of the monomers. The harmonic oscillator approximation is probably unsuitable for these low frequency modes, since they correspond to large amplitude vibrations in very shallow minima on the energy surface.

The transition structures are characterized by an imaginary frequency. The very small magnitude of the imaginary frequency for CH<sub>2</sub> + H<sub>2</sub> is consistent with the fact that the transition structure disappears at higher levels of calculation (see below and Figure 5). For the other transition structures, the imaginary frequencies are larger and are indicative of a weakly avoided crossing between the reactant and product energy surfaces. The H<sub>2</sub>-carbene or H<sub>2</sub>-silylene bending modes are relatively high in frequency, corresponding to a tight transition state. Except for CH<sub>2</sub> + H<sub>2</sub>, the transition-state frequencies resemble the products more closely than the reactants. This is in keeping with the optimized geometry which is characteristic of a late transition state: long H-H and short H<sub>2</sub>-carbene or -silylene distances (especially for CF<sub>2</sub> and SiF<sub>2</sub>).

**Energetics.** The total energies for the various equilibrium structures and transition states are listed in Table II. The calculated heats of reaction are compared with experiment in Table III; individual barrier heights and cluster well depths are collected in Tables IV and V, respectively. To simplify the comparisons and to emphasize the trends, the data are also summarized in Figure 5.

The heats of reaction (Table III) have been calculated with extended (3-21G) and polarization (6-31G\*) basis sets at the

(33) Bauschlicher C. W., Jr.; Schaefer, H. F., III; Bagus, P. S. *J. Am. Chem. Soc.* 1977, 99, 7106.

**Table II.** Total Energies<sup>a</sup>

| system                            | HF/3-21G   | HF/6-31G*  | MP2/6-31G* | MP3/6-31G* | MP4/6-31G* |
|-----------------------------------|------------|------------|------------|------------|------------|
| CH <sub>2</sub> + H <sub>2</sub>  |            |            |            |            |            |
| reactants                         | -39.77481  | -39.99920  | -40.11399  | -40.13696  | -40.14281  |
| cluster                           | -39.77699  | -40.00012  | -40.11607  | -40.13891  | -40.14465  |
| transition state                  | -39.77691  | -39.99917  | -40.12123  | -40.14298  | -40.14847  |
| product                           | -39.97688  | -40.19517  | -40.33244  | -40.34848  | -40.35208  |
| CHF + H <sub>2</sub>              |            |            |            |            |            |
| reactants                         | -138.12502 | -138.88136 | -139.17299 | -139.18720 | -139.19851 |
| transition state                  | -138.09592 | -138.85195 | -139.15894 | -139.17234 | -139.18142 |
| product                           | -138.28189 | -139.03462 | -139.33506 | -139.34683 | -139.35342 |
| CF <sub>2</sub> + H <sub>2</sub>  |            |            |            |            |            |
| reactants                         | -236.49777 | -237.78757 | -238.25376 | -238.25939 | -238.27458 |
| transition state                  | -236.41395 | -237.70228 | -238.18512 | -238.19264 | -238.20524 |
| product                           | -236.60910 | -237.89635 | -238.36244 | -238.36846 | -238.27837 |
| SiH <sub>2</sub> + H <sub>2</sub> |            |            |            |            |            |
| reactants                         | -289.60725 | -291.12661 | -291.21117 | -291.23338 | -291.23987 |
| cluster                           | -289.60875 | -291.12717 | -291.21227 | -291.23447 | -291.24089 |
| transition state                  | -289.56503 | -291.09765 | -291.19911 | -291.22114 | -291.22631 |
| product                           | -289.68698 | -291.22513 | -291.30703 | -291.32541 | -291.33011 |
| SiHF + H <sub>2</sub>             |            |            |            |            |            |
| reactants                         | -388.00462 | -390.05873 | -390.31823 | -390.33208 | -390.34260 |
| cluster                           | -388.00556 | -390.05904 | -390.31874 | -390.33259 | -390.34308 |
| transition state                  | -387.93421 | -390.00060 | -390.27316 | -390.28824 | -390.29741 |
| product                           | -388.07406 | -390.14840 | -390.39971 | -390.41053 | -390.41830 |
| SiF <sub>2</sub> + H <sub>2</sub> |            |            |            |            |            |
| reactants                         | -486.42359 | -489.01150 | -489.44756 | -489.45299 | -489.46713 |
| transition state                  | -486.30327 | -488.90226 | -489.34530 | -489.35305 | -489.36615 |
| product                           | -486.47324 | -489.08181 | -489.50468 | -489.50825 | -489.51920 |

<sup>a</sup> In au, 1 au = 2625.5 kJ mol<sup>-1</sup>.**Table III.** Heats of Reaction<sup>a</sup>

| level                              | CH <sub>2</sub> + H <sub>2</sub> | CHF + H <sub>2</sub> | CF <sub>2</sub> + H <sub>2</sub> | SiH <sub>2</sub> + H <sub>2</sub> | SiHF + H <sub>2</sub> | SiF <sub>2</sub> + H <sub>2</sub> |
|------------------------------------|----------------------------------|----------------------|----------------------------------|-----------------------------------|-----------------------|-----------------------------------|
| HF/3-21G                           | -532                             | -412                 | -292                             | -209                              | -182                  | -131                              |
| HF/6-31G*                          | -515                             | -403                 | -286                             | -259                              | -236                  | -185                              |
| MP2/6-31G*                         | -574                             | -426                 | -285                             | -252                              | -214                  | -150                              |
| MP3/6-31G*                         | -555                             | -419                 | -286                             | -241                              | -206                  | -145                              |
| MP4/6-31G*                         | -549                             | -407                 | -272                             | -237                              | -199                  | -137                              |
| ΔZPE                               | 52                               | 49                   | 46                               | 23                                | 25                    | 24                                |
| ΔH <sub>f</sub> <sup>0</sup> , 0 K |                                  |                      |                                  |                                   |                       |                                   |
| theor                              | -497                             | -358                 | -226                             | -214                              | -174                  | -113                              |
| exptl                              | -496 ± 2                         | -351 ± 25            | -259 ± 4                         | -204 ± 6                          | -199 ± 25             | -195 ± 20                         |

<sup>a</sup> In kJ mol<sup>-1</sup>.**Table IV.** Barrier Heights<sup>a</sup>

| level      | CH <sub>2</sub> + H <sub>2</sub> | CHF + H <sub>2</sub> | CF <sub>2</sub> + H <sub>2</sub> | SiH <sub>2</sub> + H <sub>2</sub> | SiHF + H <sub>2</sub> | SiF <sub>2</sub> + H <sub>2</sub> |
|------------|----------------------------------|----------------------|----------------------------------|-----------------------------------|-----------------------|-----------------------------------|
| HF/3-21G   | 1                                | 76                   | 220                              | 115                               | 185                   | 317                               |
| HF/6-31G*  | 3                                | 77                   | 224                              | 77                                | 153                   | 287                               |
| MP2/6-31G* | -13                              | 39                   | 180                              | 35                                | 118                   | 269                               |
| MP3/6-31G* | -11                              | 39                   | 175                              | 35                                | 115                   | 262                               |
| MP4/6-31G* | -10                              | 45                   | 182                              | 38                                | 119                   | 265                               |
| ΔZPE/3-21G | 18                               | 19                   | 15                               | 13                                | 11                    | 8                                 |

<sup>a</sup> In kJ mol<sup>-1</sup>.

Hartree-Fock level and with electron correlation taken into account by Møller-Plesset perturbation theory (MP2, MP3, and MP4SDQ4). The effect of d orbitals (3-21G → 6-31G\*) is small for carbon, but larger for silicon. The electron correlation contribution is relatively small, except for CH<sub>2</sub>, which has a low-lying excited state, and for SiF<sub>2</sub>, which has very polar Si-F bonds. The change in zero-point energy is sizable and reflects the difference between the vibrational frequencies of H<sub>2</sub> and two C-H or Si-H stretches.

Experimental values for the heats of formation (0 K) for CH<sub>2</sub>, SiH<sub>2</sub>, CF<sub>2</sub>, and SiF<sub>2</sub> are 429.3 ± 2,<sup>34</sup> 248.1 ± 6,<sup>35</sup> -186.6 ± 2,<sup>36</sup>

(34) Hayden, C. C.; Neumark, D. M.; Shobatake, K.; Sparks, R. K.; Lee, Y. T. *J. Chem. Phys.* **1982**, *76*, 3607.

(35) Bell, T. N.; Perkins, K. A.; Perkins, P. G. *J. Chem. Soc., Faraday Trans. 1* **1981**, *77*, 1779.

(36) Carlson, G. A. *J. Phys. Chem.* **1971**, *75*, 1625. Schug, K. P.; Wagner, H. G. *Ber. Bunsenges, Phys. Chem.* **1978**, *82*, 719.

**Table V.** Cluster Well Depths<sup>a</sup>

| level      | CH <sub>2</sub> + H <sub>2</sub> <sup>b</sup> | SiH <sub>2</sub> + H <sub>2</sub> | SiHF + H <sub>2</sub> |
|------------|---|-----------------------------------|-----------------------|
| HF/3-21G   | 5.1   | 3.9                               | 2.5                   |
| HF/6-31G*  | 2.4   | 1.5                               | 0.8                   |
| MP2/6-31G* | 5.5   | 2.9                               | 1.3                   |
| MP3/6-31G* | 5.1   | 2.8                               | 1.3                   |
| MP4/6-31G* | 4.8   | 2.7                               | 1.3                   |

<sup>a</sup> In kJ mol<sup>-1</sup>. <sup>b</sup> See text.

and -587.4 ± 1<sup>37</sup> kJ mol<sup>-1</sup>, respectively. The tabulated value for CHF is a linear interpolation,<sup>32</sup> ΔH<sub>f</sub><sup>0</sup> (0 K) = 121 ± 25 kJ mol<sup>-1</sup>; no value is listed for SiHF, but a similar interpolation yields -170

(37) Farber, M.; Srivastava, R. D. *J. Chem. Soc., Faraday Trans. 1* **1978**, *74*, 1089.

(38) A more recently determined heat of formation of CF<sub>2</sub> was used in the interpolation.

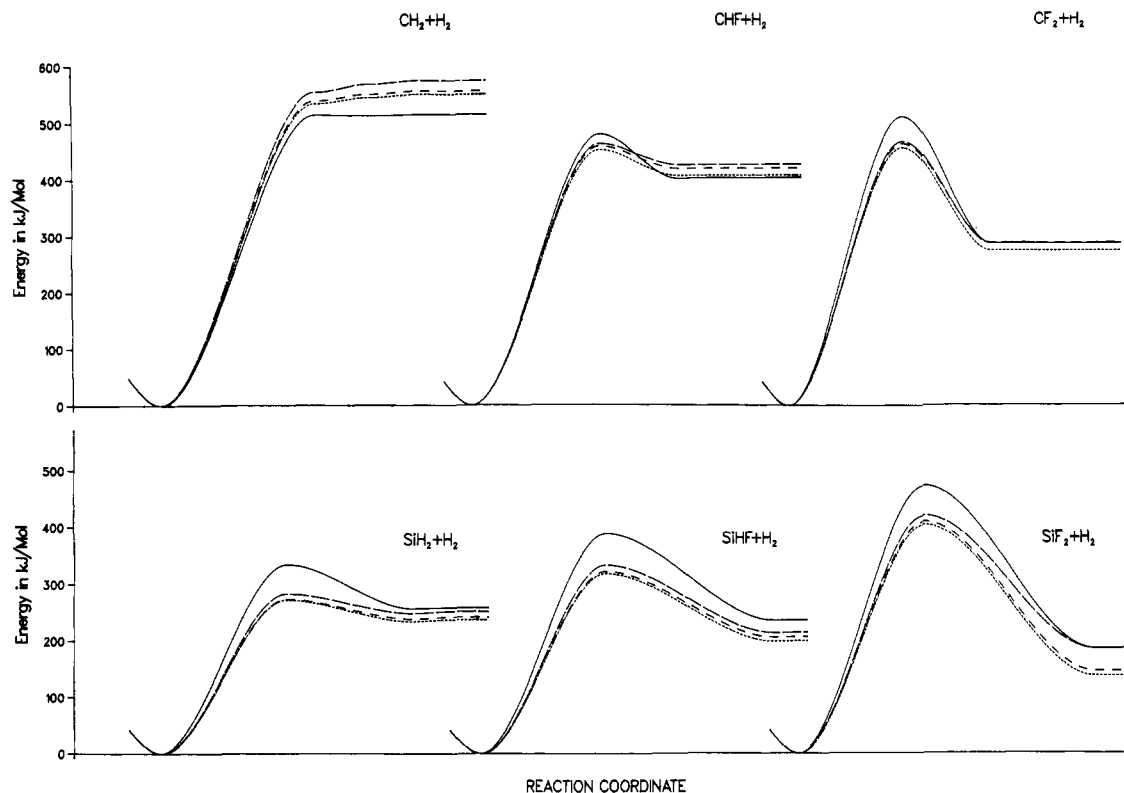


Figure 5. Energy profiles along the reaction path for insertion: HF/6-31G\* (solid line), MP2/6-31G\* (long dashes), MP3/6-31G\* (medium dashes), and MP4SDQ/6-31G\* (short dashes).

$\pm 25 \text{ kJ mol}^{-1}$ . Other sources of uncertainty include the heats of formation for  $\text{SiH}_3\text{F}$  and  $\text{SiH}_2\text{F}_2$ ,<sup>32</sup> also based on linear interpolations.<sup>39</sup> The theoretical heats of reaction for  $\text{CH}_2 + \text{H}_2$  and  $\text{SiH}_2 + \text{H}_2$  are in good agreement with experiment. For substituted carbenes and silylenes, there is a  $\sim 15 \text{ kJ mol}^{-1}$  error per C–F bond and a  $\sim 40 \text{ kJ mol}^{-1}$  error per Si–F bond. Fluorine-containing molecules are notoriously difficult to calculate accurately but also pose serious problems experimentally.

The calculated barrier heights for insertion are collected in Table IV. Experimentally,  $\text{CH}_2 + \text{H}_2$  has no barrier. The minute barrier found on the Hartree–Fock energy surface disappears when correlation energy is added; inclusion of zero-point energy restores a small barrier. For silylene insertion, a barrier of  $23 \pm 4 \text{ kJ mol}^{-1}$  has been obtained experimentally.<sup>22</sup> The calculated barrier is much too high at the Hartree–Fock level but is in reasonable agreement when electron correlation is included. The present results are comparable to those of Gordon.<sup>18</sup> Schaefer et al.<sup>19</sup> have performed more extensive calculations using MCSCF methods with larger basis sets, augmented by CISD plus size consistency corrections, and found a barrier of  $28 \text{ kJ mol}^{-1}$ .

With fluorine substitution, there is a large increase in the barrier height at all levels of calculation, both for the carbenes and for the silylenes. The first fluorine increases the barrier by ca.  $80 \text{ kJ mol}^{-1}$  and the second by an additional  $\sim 130 \text{ kJ mol}^{-1}$ . A similar increase in the barrier is found for hydroxy substitution<sup>23</sup> in the reaction  $\text{HCOH} + \text{H}_2 \rightarrow \text{CH}_3\text{OH}$ . The inclusion of d orbitals is more important for silicon than for carbon; correlation corrections lower the barriers by  $30\text{--}40 \text{ kJ mol}^{-1}$ , except for  $\text{CH}_2$  and  $\text{SiF}_2$  where the change is only  $10\text{--}20 \text{ kJ mol}^{-1}$ . Neither the basis set effects nor the correlation energy corrections are large enough to alter the trend of large increases in the barrier height

(39) The heats of formation of fluoromethanes have been critically examined by Rodgers<sup>40</sup> and also reviewed by Benson.<sup>41</sup> In the series  $\text{CH}_4$  to  $\text{CF}_4$ , the heats of formation changes by smoothly varying increments. Recent experiments<sup>42</sup> on  $\text{SiH}_3\text{F}$ ,  $\text{SiH}_2\text{F}_2$ , and  $\text{SiHF}_3$  do not yield similar smooth trends in the heats of formation. The heat of formation of  $\text{SiF}_3$  obtained in an analogous study<sup>37</sup> has also been criticized.<sup>7</sup> In light of these difficulties, the simple linear interpolation used in the JANAF tables<sup>32</sup> may be a more uniform approximation. An ab initio molecular orbital study has been undertaken to obtain theoretical estimates for the heats of formation of the fluorosilanes.<sup>43</sup>

with greater fluorine substitution.

For three of the systems, loose clusters could be found along the reaction path for insertion. The  $\text{CH}_2 + \text{H}_2$  structure optimized at the Hartree–Fock level is not stable at the Møller–Plesset level. The MP/6-31G\* energy of the HF/6-31G\* optimized “cluster” is higher than the MP/6-31G\* energy of the HF/6-31G\* optimized “transition state”. This is consistent with the absence of a barrier to  $\text{CH}_2$  insertion at the post Hartree–Fock level. Attempts to locate clusters for CHF and  $\text{CF}_2$  were unsuccessful, suggesting that these clusters either do not exist or are only very weakly bound. The  $\text{SiH}_2 + \text{H}_2$  cluster optimized at HF/6-31G\* has a depth of  $2.7 \text{ kJ mol}^{-1}$  at MP4/6-31G\* (optimization at a correlated level with a larger basis set increases the well depth by a few  $\text{kJ mol}^{-1}$ ).<sup>44</sup> The well for SiHF is only half as deep and occurs at a larger separation. Extrapolation to  $\text{SiF}_2$  implies that the binding for an  $\text{SiF}_2 + \text{H}_2$  cluster along the reaction path is very small, if such a cluster exists. Inspection of the trends in the orbital energies and the dipole moments suggests that the clusters are weak donor–acceptor complexes rather than dipole–quadrupole interactions.

## Discussion

The large increase in the barrier height with greater fluorine substitution could be explained in a number of ways. One approach is to divide the barrier into contributions from the distortion of the monomers and contributions from the interaction of the distorted monomers. Figure 3 reveals systematic changes in the transition structure geometries, suggesting that the increases in the barrier height are primarily due to greater distortion of the monomers in the transition state. For the series  $\text{CH}_2$ , CHF,  $\text{CF}_2$ , and  $\text{SiH}_2$ , SiHF,  $\text{SiF}_2$ , a total of 1, 24, 84 and 165, 173, 202  $\text{kJ mol}^{-1}$  is required to distort the monomers from equilibrium to their transition-state geometries (HF/3-21G). The largest contribution

(40) Rodgers, A. S.; Chao, J.; Wilhoit, R. C.; Zwolinski, B. J. *J. Phys. Chem. Ref. Data* 1974, 3, 117.

(41) Benson, S. W. *J. Phys. Chem.* 1981, 85, 3375.

(42) Farber, M.; Srivastava, R. D. *Chem. Phys. Lett.* 1977, 51, 307.

(43) Schlegel, H. B. *J. Phys. Chem.*, in press.

(44) Gordon, M. S.; Binkley, J. S., private communication.

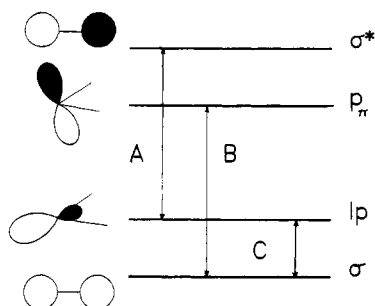


**Figure 6.** Dominant orbital interactions in the transition state: (A) two-electron stabilization between the carbene or silylene lone pair (1p) and the H<sub>2</sub>  $\sigma^*$ , (B) two-electron stabilization between the empty carbene or silylene p orbital ( $p\pi$ ) and the H<sub>2</sub>  $\sigma$ , (C) four-electron destabilization between the lone pair and  $\sigma$ . Fluorine substitution lowers the lone pair and slightly raises the  $p\pi$  orbital energies.

is due to H<sub>2</sub> stretching. These values follow the trend in barrier heights for the carbenes but not the silylenes, and the magnitudes are not sufficient to explain the large increase in the barriers.

If the barrier heights cannot be rationalized in terms of the energy required to distort the reactants to their transition structure geometries, then the electronic interaction of these fragments must govern the trends in the barrier heights. At the HF/3-21G level, the interaction energies between the monomers are 0, 52, and 136 and -50, 12, and 115 kJ mol<sup>-1</sup> for the series CH<sub>2</sub>, CHF, and CF<sub>2</sub> and SiH<sub>2</sub>, SiHF, and SiF<sub>2</sub>, respectively (obtained by subtracting the distortion energies from the barrier heights). A simple perturbational molecular orbital (PMO) model can be constructed to explain the trends in the interaction energies and therefore the changes in the barrier heights with fluorine substitution. The main orbitals involved in the insertion reaction<sup>3</sup> are the  $\sigma$  and  $\sigma^*$  of the hydrogen interacting with the occupied  $\sigma$ -type lone pair (1p) and the unoccupied  $\pi$ -type p orbital ( $p\pi$ ) on the carbene or silylene. The approximate shapes and energies are shown in Figure 6. The primary result of electronegative substituents such as fluoro, hydroxy, or methoxy is to lower the lone pair energy through inductive effects. In addition, the empty  $p\pi$  orbital is raised slightly by antibonding interactions with the filled fluorine  $\pi$ -type lone pairs. The widening of the 1p- $p\pi$  (HOMO-LUMO) gap is also responsible for the large increase in the singlet-triplet separation

on fluorine substitution.<sup>45</sup> The transition structure is stabilized by 1p- $\sigma^*$  two-electron interaction (A in Figure 6) and by a  $\sigma$ - $p\pi$  two-electron interaction (B). Fluorine substitution lowers the energy of 1p and raises  $p\pi$ , widening the gap for both interactions, thus decreasing the stabilization in the transition state and increasing the barrier. Even more important than the stabilizing interactions is the four-electron destabilizing interaction between 1p and  $\sigma$  (C in Figure 6). Fluorine substitution lowers 1p, closing the gap, increasing the destabilization, and increasing the barrier. Since the net effect of fluorine is the same in all three interactions, the increase in the barrier height is quite dramatic.

## Conclusions

At all levels of calculation, fluorine substitution leads to a large increase in the barrier height for carbene and silylene insertions into hydrogen molecule. To the extent that H<sub>2</sub> is representative of a covalent single bond, CF<sub>2</sub> and SiF<sub>2</sub> insertions will not occur, and SiHF insertions will be difficult. This explains, in part, why SiF<sub>2</sub> is relatively inert in the gas phase. On the basis of PMO analysis, the behavior of methoxy-substituted compounds should be quite similar to the fluoro species. From the magnitude of the insertion barriers, we can also deduce that SiH<sub>3</sub>F will form SiH<sub>2</sub> + HF rather than SiHF + H<sub>2</sub> during pyrolysis, similarly SiH<sub>2</sub> F<sub>2</sub> → SiH<sub>2</sub> + F<sub>2</sub> or SiHF + HF rather than SiF<sub>2</sub> + H<sub>2</sub>. Insertion into polar bonds may be more facile than insertion into H<sub>2</sub>, since the silylene or carbene can be reoriented to reduce the four-electron repulsion that appears to control the barrier height. For insertions into multiple bonds, additional interactions must be considered and the trends may be different.

**Acknowledgment.** This work was supported by a grant from the National Science Foundation and the donors of the Petroleum Research Fund, administered by the American Chemical Society. We thank the Computer Services Center at Wayne State University for a generous allocation of computer time.

**Registry No.** CH<sub>2</sub>, 2465-56-7; CHF, 13453-52-6; CF<sub>2</sub>, 2154-59-8; SiH<sub>2</sub>, 13825-90-6; SiHF, 50561-30-3; SiF<sub>2</sub>, 13966-66-0; H<sub>2</sub>, 1333-74-0.

(45) For alternate but compatible explanations see: (a) Harrison, J. F.; Liedtke, R. C.; Liebman, J. F. *J. Am. Chem. Soc.* **1979**, *101*, 7162 and references cited. (b) Feller, D.; Borden, W. T.; Davidson, E. R. *Chem. Phys. Lett.* **1980**, *71*, 22.